886 *Macromolecules* **2011**, *44*, 886–893
DOI: 10.1021/ma1026466

Macromolecules
ARTICLE

The Missing Lactam-Thermoresponsive and Biocompatible Poly(*N*-vinylpiperidone) Polymers by Xanthate-Mediated RAFT Polymerization

Nga Sze Ieong,[†] Martin Redhead,[‡] Cynthia Bosquillon,[‡] Cameron Alexander,[‡] Malcolm Kelland,[§] and Rachel K. O'Reilly*,[†]

[†]*Department of Chemistry, University of Warwick, Gibbet Hill Road, Coventry CV4 7AL, U.K.,* [‡]*School of Pharmacy, University of Nottingham, University Park, Nottingham NG7 2RD, U.K., and* [§]*Department of Mathematics and Natural Sciences, Faculty of Science and Technology, University of Stavanger, 4036 Stavanger, Norway*

Received November 25, 2010; Revised Manuscript Received January 10, 2011

ABSTRACT: A new polymer poly(*N*-vinylpiperidone) (PVPip) (**2**$_x$, M_n^{NMR} 4.5−83 kDa) has been prepared by reversible addition−fragmentation chain-transfer (RAFT) polymerization using a xanthate as a chain-transfer agent. These polymers all exhibited sharp reversible cloud points (in the range 87 and 68 °C) which depended on the molecular weight of the polymer and showed no apparent hysteresis. Furthermore, cytotoxicity studies of the PVPip showed that the polymer is noncytotoxic. Chain extension of PVPip$_{62}$ with vinyl acetate afforded well-defined amphiphilic diblock copolymers: poly(*N*-vinylpiperidone)$_x$-*block*-poly(vinyl acetate)$_y$ (PVPip$_x$-*b*-PVAc$_y$) (for **3**, x:y = 62:21; for **4**, x:y = 62:32). Both **3** and **4** exhibit phase transitions of 62 and 55 °C, respectively, in water, with the latter showing evidence of a slight hysteresis. Direct dissolution of **3** in nanopure water at 1 mg/mL gave spherical micelles (ca. 24 nm), as confirmed by DLS, TEM, and AFM analysis, which could be reversibly disassembled upon heating above the cloud point of the diblock. The block copolymer **4** was hydrolyzed under basic conditions to give the double hydrophilic biocompatible diblock copolymer poly(*N*-vinylpiperidone)$_{62}$-*block*-poly(vinyl alcohol)$_{32}$ (**5**).

Introduction

Recently, significant scientific interest has been devoted to the development of stimuli-responsive or "smart" polymers. In particular, thermoresponsive materials[1−3] which can undergo fast and reversible solubility changes in response to a temperature trigger have received much focus due to their promising potential in a wide range of applications including controlled drug delivery,[4−8] separation processes,[9] and tissue engineering.[10] Most of these thermosensitive materials are based on water-soluble polymers with a lower critical solution temperature (LCST)—a critical temperature below which the polymer is soluble and above which phase separation occurs.[11] To date, poly(*N*-isopropylacrylamide) (PNIPAAm), which exhibits an LCST at 32 °C, has remained the most extensively studied class of thermoresponsive polymer.[12,13] By varying the amounts of hydrophilic/hydrophobic comonomer, PNIPAAm-based polymers with tunable LCSTs can be readily achieved.[14] The excellent stimuli-responsive properties of PNIPAAm, which includes an LCST close to body temperature and more importantly being relatively insensitive to other environmental stimuli such as small changes in concentrations, pH, and/or varying molecular weights,[13,15] have led to its extensive exploration and use as a thermosensitive materials for biomedical applications.[2] However, despite the widespread study of PNIPAAm, these polymers have inherent disadvantages which include a strong hysteresis and a high melting point, and also for low molecular weight polymers the nature of the end group can significantly affect the responsive properties (although this final point is true for other polymers, it is important to note in PNIPAAm as its LCST is generally considered to be independent of molecular weight which may not be the case for short polymer chains where end groups have an effect).[16,17] Subsequently, polymers containing short oligo(ethylene glycol) side chains have been explored and are promising alternatives to PNIPAAm for applications in biomedicine.[18,19] For example, seminal work by Lutz et al. in 2006 reported that the biocompatible PEGylated polymer (poly(2-(2-methoxyethoxy)ethyl) methacrylate-*co*-oligo(ethylene glycol) methacrylate) (P(MEO$_2$MA-*co*-OEGMA)), prepared by atom transfer radical polymerization (ATRP), exhibited not only an LCST similar to PNIPAAm but also no apparent hysteresis and cloud point which was independent of the chain length, thus making this polymer a potential alternative to PNIPAAm.[20,21] Furthermore, the incorporation of hydrophobic and labile 5, 6-benzo-2-methylene-1,3-dioxepane (BMDO) linkages in the (P(MEO$_2$MA-*co*-OEGMA)) polymer backbone not only retained the superior thermoresponsive and biocompatibility properties but also rendered them biodegradable.[22] Another interesting class of biodegradable and thermoresponsive polymer is the poly(2-oxazoline)s, which can be prepared by cationic ring-opening polymerization.[23] These polymers display sharp LCST transitions which can be readily tuned by changing the molecular weights or comonomer compositions to modify the hydrophilic/hydrophobic nature of the final copolymer.[24,25] Indeed, recent work by Hoogenboom and Schubert demonstrated that the LCST could be easily tuned by rational design of the polymer compositions and molecular weights.[26] Another important family of thermoresponsive and also biocompatible polymers are the poly(*N*-vinyllactams). While the 5-membered ring polylactam (poly(*N*-vinylpyridone), PVP) does not possess an LCST below 100 °C,[27,28] the 7-membered ring analogue,

*To whom correspondence should be addressed.

 Published on Web 01/28/2011

namely poly(*N*-vinylcaprolactam) (PVCap), has an LCST close to physiological temperature (34−37 °C), making it the subject of much current interest.[27−30] Homopolymers and copolymers of both PVCap and PVP are often prepared by controlled radical polymerization techniques such as macromolecular design via interchange of xanthates (MADIX)/reversible addition−fragmentation chain transfer (RAFT),[31−36] nitroxide-mediated,[37] atom transfer radical polymerization (ATRP),[38] and cobalt-mediated radical polymerization.[39] In contrast to the vast amount of scientific literature on the preparation and the study of the stimuli-responsive behavior of the 5-membered and less so the 7-membered ring poly(*N*-vinyllactam) analogues,[29,40−45] there have been no reports so far on the homopolymerization of the 6-membered ring analogue, *N*-vinylpiperidone (VPip). Indeed in 2010, the first report of the copolymerization of the 6-membered ring monomer using free radical polymerization was reported.[46] It is proposed that these new *N*-vinylpiperidone polymers would display intermediate LCST/cloud point values and also analogous biocompatibility as the previously reported PVP and PVCap and hence find application in biomedical and materials applications. In this paper, we describe for the first time the controlled homopolymerization of *N*-vinylpiperidone using MADIX/RAFT polymerization with a xanthate as a chain-transfer agent. These new polymers (PVPip) were then used as macromolecular chain-transfer agents to form an amphiphilic diblock copolymer (poly(*N*-vinylpiperidone)-*b*-poly(vinyl acetate)) which could undergo thermoreversible solution self-assembly to form spherical micelles. Furthermore, these polymers could be deprotected to form a fully biocompatible thermosensitive polymer, poly(*N*-vinylpiperdone)-*b*-poly(vinyl alcohol). Preliminary thermoresponsive behavior of these novel materials will also be discussed.

Experimental Section

Materials and Methods. 2,2′-Azobis(2-methylpropionitrile) (AIBN, Molekular) was recrystallized from methanol and stored at −35 °C in the dark. Ethyl 2-(ethoxycarbonothioylthio)propanoate (**1**) was synthesized according to the literature procedures.[47] *N*-Vinylpiperidone (VPip) was donated by BASF, stored in the desiccator, and sublimed before use. 1,4-Dioxane was dried over CaH_2 and distilled under reduced pressure prior to use. Vinyl acetate was dried over CaH_2, distilled under static vacuum, and then stored at −35 °C in the dark. All other reagents were purchased from Sigma-Aldrich and were used without further purification.

^{1}H and ^{13}C{^{1}H} spectra were recorded with a Bruker DPX-400 spectrometer using $CDCl_3$ or D_2O. Chemical shifts are reported in ppm (δ) relative to $CHCl_3$ (7.26 ppm for ^{1}H and 77.2 ppm for ^{13}C{^{1}H}) and H_2O (4.79 ppm for ^{1}H) as internal references. Gel permeation chromatography (GPC) data were obtained on a PL GPC 50 integrated GPC system with a PL-AS RT autosampler and a Varian 390-LC detector suite with DRI and viscometry. Three mixed D, 5 μm columns (one guard and two main) were used at 50 °C with dimethylformamide (DMF) with 1% LiBr as the eluent at a flow rate of 1 mL/min. All molecular weights were calculated relative to PMMA standards. For the homopolymers $\mathbf{2}_{36,51,62}$ and block copolymers **3**−**5** as well as polymerization kinetics analyses, GPC data were also obtained on a PL GPC 50 integrated with a DRI and a UV detector. One PL gel mixed E, 3 μm column and one guard column were used at 30 °C with 1,1,1,3,3,3-hexafluoro-2-propanol (HFIP) with 0.05% w/v potassium trifluoroacetate as the eluent at a flow rate of 0.5 mL/min. All molecular weights were calculated relative to PMMA standards (M_p 0.6 −30.5 kDa). For the homopolymers $\mathbf{2}_{85,209,652}$, GPC data were also obtained on a PL GPC 50 integrated GPC with a DRI and a UV detector. One Waters Styragel HT column and one guard column were used at 30 °C with HFIP with 0.05% w/v potassium trifluoroacetate as the eluent at a flow rate of 1.0 mL/min. All molecular weights were calculated relative to PMMA standards (M_p 5.7 −467.4 kDa).

The DLS instrumentation consisted of a Malvern Zetasizer NanoS instrument operating at 25−80 °C with a 4 mW He−Ne 633 nm laser module. Measurements were made at a detection angle of 173° (backscattering), and Malvern DTS 5.02 software was used to analyze the data. The data were processed by cumulants analysis of the experimental correlation function, and spherical micelle diameters were calculated from the computed diffusion coefficients using the Stokes−Einstein equation. Each reported measurement was the average of three runs.

Transmission electron microscopy (TEM) samples were prepared by drop deposition onto copper/carbon grids that had been treated with oxygen plasma to increase the surface hydrophilicity. The particles were stained using a dilute 3% solution of uranyl acetate. Micrographs were collected at magnifications varying from 12 to 100 K and calibrated digitally. Histograms of number-average particle diameters (D_{av}) and standard deviations were generated from the analysis of a minimum of 100 particles from at least three different micrographs using Image J software.

A Veeco MultiMode AFM was used with a Nanoscope IIIa controller and Quadrex module (Digital Instruments, Veeco Metrology Group; Santa Barbara, CA). The tips were silicon with nominal force constant and resonant frequency of 3.5 N/m and 75 kHz (NSC18/no Al from MikroMasch). The samples were prepared for AFM analysis by drop deposition of ∼0.1 mL of sample at a concentration of 1 mg/mL onto freshly cleaved mica and air-dried overnight. Average height (H_{ave}) of micelles was calculated based on at least 50 particles. Lower critical solution temperature (LCST)/cloud point measurements were analyzed using a Perkin-Elmer UV/vis Spectrometer (Lambda 35) equipped with a Peltier temperature controller at 500 nm with a heating/cooling rate of 1 °C/min. An average of at least two cycles were recorded for each sample. Infrared (IR) spectra were obtained on a Perkin-Elmer Spectrum 100 ATR FT-IR spectrometer. Critical aggregate concentration (CAC) determination was performed according to a previously published method employing *N*-phenyl-1-naphthylamine (PNA) as a fluorescence probe using a Cary Eclipse single-beam fluorimeter.[48] DSC measurements were performed on a Mettler Toledo, HP DSC827 with analysis performed using Mettler Toledo STARe software v9.20. The samples were run at a heating rate of 10 °C/min, and the glass transition temperatures were taken as the midpoint of the inflection tangent.

Polymerization of *N*-Vinylpiperidone (VPip) Using CTA 1. As a representative example, in an inert atmosphere glovebox, VPip (3.00 g, 24 mmol), CTA **1** (16 mg, 0.072 mmol) and AIBN (0.62 mL of 1.88 mg/mL dioxane) were dissolved in 1,4-dioxane (5.4 mL) in a vial. The resulting solution was then introduced into a Schlenk tube equipped with a Young's tap, sealed under nitrogen, and then taken out of the glovebox. The reaction mixture was then allowed to polymerize at 70 °C for typically 10 h, after which an aliquot was taken from the mixture for ^{1}H NMR conversion analysis. Conversions were calculated using ^{1}H NMR spectroscopy by comparing the integrations of the heterocycle signals on the VPip monomer (δ = 3.57 and 2.45 ppm) with those of the corresponding signals of the polymer backbone (δ = 3.05 and 2.28 ppm). The light yellow solution was then quenched with liquid nitrogen. Poly(*N*-vinylpiperidone) (PVPip) was recovered as an off-white powder (1.7 g, ca. 91% based on 62% conversion) after precipitation into diethyl ether multiple times until the residual monomer was less than 0.2%. Representative characterization data for $\mathbf{2}_{209}$: ^{1}H NMR (400 MHz, $CDCl_3$): δ = 4.57 (−NC*H*, br, 1H), 4.08 (−OCH_2CH$_3$, end group), 3.05 (−NCH_2−, br, 2H), 2.34−2.21 (O=C−CH_2−, br, 2H), 1.83−1.43 (−CH_2− on heterocycle, −CH_2− on polymer backbone, br, 6H). ^{13}C {^{1}H} NMR (125 MHz, $CDCl_3$): δ = 169.9 (−*C*=O), 45.3, 44.0 (−N*C*H on polymer backbone), 40.8

(−NCH_2−), 32.7 (O=C−CH_2−), 22.9, 21.2, 21.0, 20.9 (−CH_2− on heterocycle, −CH_2− on polymer backbone). M_n^{NMR} ($CDCl_3$) = 26 kDa, M_n^{GPC}(DMF) = 8.2 kDa, M_w/M_n = 1.58. M_n^{GPC}(HFIP) = 30.0 kDa, M_w/M_n = 1.59. DSC of $PVPip_x$: T_g = 94−98 °C.

Chain Extension of PVPip with Vinyl Acetate (VAc) To Afford Poly(*N*-vinylpiperidone)-*block*-poly(vinyl acetate) (PVPip-*b*-PVAc). As a representative example, $\mathbf{2_{62}}$ (M_n^{NMR} = 8.1 kDa, M_w/M_n (DMF GPC) = 1.25, M_w/M_n (HFIP GPC) = 1.28, 0.201 g, 0.0248 mmol), VAc (1.3 mL, 0.0141 mol), and AIBN (0.1 mL of 4.20 mg/mL solution in 1,4-dioxane, 0.0026 mmol) were dissolved in 1,4-dioxane (18 mL, [VAc] = 0.78 M) in an inert atmosphere glovebox. The resulting solution was transferred to a Schlenk tube equipped with a Young's tap, sealed under nitrogen, and then taken out of the glovebox. The polymerization was then carried out at 60 °C for 68 h, after which an aliquot was withdrawn from the reaction mixture for ^{1}H NMR conversion analysis—determined by comparing the integrations of the vinyl (δ = 7.25 ppm) and the −CH_3 (δ = 2.11 ppm) proton signals of the VAc monomer with those of the −CH_3 proton peaks (δ = 2.00 ppm) of the resulting polymer. The polymerization was quenched with liquid nitrogen and subsequently precipitated into diethyl ether twice, giving an off-white fluffy material with a clear colorless supernatant which was then carefully decanted. PVPip-*b*-PVAc was obtained as a transparent sticky solid after drying under high vacuum for 2 days. Characterization of **4**: ^{1}H NMR (400 MHz, $CDCl_3$): δ = 4.84 (−C*H*− of PVAc, br), 4.54 (−NC*H*− of PVPip, br), 4.11(−OCH_2-CH_3, end group), 3.02 (−NCH_2−, br, PVPip), 2.34−2.18 (O=C−CH_2−, br, PVPip), 2.00 (−CH_3, br, PVAc), 1.83−1.40 (−CH_2− on PVPip heterocycle, −CH_2− on PVPip and PVAc polymer backbone, br). M_n^{NMR} ($CDCl_3$) = 10.8 kDa, M_n^{GPC}-(DMF) = 7.4 kDa, M_w/M_n = 1.55. M_n^{GPC}(HFIP) = 11.4 kDa, M_w/M_n = 1.27. DSC of **4**: T_g = 43 °C (PVAc), 88 °C (PVPip).

Hydrolysis of 4 To Form 5. A solution of **4** (0.16 g, 1.52×10^{-2} mmol), ethylpyridine hypophosphite (EPHP) (0.124 g, 0.67 mmol), and AIBN (1.09 mg, 6.64×10^{-3} mmol) in toluene (ca. 4 mL) was degassed by freeze−pump−thaw cycle five times. The resulting reaction mixture was then sealed under nitrogen and heated in an oil bath at 100 °C for 12 h, after which it was then concentrated in vacuo and immediately precipitated into diethyl ether two times to give **4′** as a white fluffy solid (0.130 g, 81% yield) after drying under high vacuum for 2 days. The successful removal of the xanthate end group was confirmed by the disappearance of the GPC (DMF) trace as analyzed at UV 280 nm as well as the overlapping RI traces relative to its precursor **4** (M_n^{GPC}(DMF) = 5.5 kDa, M_w/M_n = 1.58). To a rapidly stirring solution of the above polymer **4′** (0.125 g in 12 mL methanol) was added KOH (12 mL of 20 mg/mL solution in methanol). After stirring for 12 h, the reaction mixture was concentrated in vacuo, diluted with nanopure water, and dialyzed against nanopure water for 2 days (MWCO = 6−8 kDa) to remove any methanol and salts. The hydrolyzed polymer **5** was recovered as a fluffy white powder after freeze-drying for 2 days and then stored in the desiccator (0.10 g, 80% yield). ^{1}H NMR (400 MHz, D_2O): δ = 4.51 (−C*H*− of PVPip, br), 4.05 (−C*H*− of PVOH, br), 3.18 (−NCH_2− of PVPip, br), 2.50−2.00 (O=C−CH_2−, br, PVPip), 1.95−1.00 (−CH_2− on PVPip heterocycle, −CH_2− on PVOH and PVPip polymer backbone, br). M_n^{GPC}(DMF) = 3.9 kDa, M_w/M_n = 1.58. M_n^{GPC}(HFIP) = 10.7 kDa, M_w/M_n = 1.26. DSC of **5**: T_g = 89 °C.

Self-Assembly of $PVPip_{62}$-*b*-$PVAc_{21}$ (3) and $PVPip_{62}$-*b*-$PVAc_{32}$ (4). As a representative example, the diblock copolymer **3** was directly dissolved in nanopure water (at 1 mg/mL). The resulting mixture was then stirred until all the diblock copolymer unimers have been dissolved, after which it was allowed to age for 1 week before passing through a 0.45 μm nylon filter to remove dust prior to further studies.

Cytotoxicity Studies. *Lactose Dehydrogenase (LDH) Assay.* Calu3 (ATCC, Rockville, MD) cells were grown from passage 35 using Dulbecco's modified Eagle's medium nutrient mixture F-12 Ham supplemented with 10% fetal bovine serum (FBS), 100 UI/mL penicillin, 100 μg/mL streptomycin, 2 mM L-glutamine, and 1% v/v nonessential amino acids (all components from Sigma-Aldrich, Poole, UK). Calu3 cells were seeded onto 96-well plates at a density of 15 000 cells per well and incubated overnight to attach. Once attached, the growth medium was removed and replaced with growth medium containing heat inactivated FBS, with lanes also containing either; P(IP) (M_n 10 kDa) of varying concentrations between 0.0005 and 1% w/v, a control lane with 4% Triton X-100, and a lane of media without cells to determine the background. The cells were then incubated for 4 h, centrifuged at 250*g* at 4 °C for 4 min, and 100 μL of growth media containing heat-inactivated FBS was added to each well. 100 μL of media was then taken from each well and placed into a fresh 96-well plate. 100 μL of CytoTox-ONE reagent (Promega) was then added to each well on the new plate, and the plate was incubated at room temperature for 15 min protected from light. CytoTox-ONE reagent contains lactate, NAD+, ATP, diaphorase, and rezazurin. Following incubation, 50 μL of stop solution (Promega) was added to each well and the plates were read on a TECAN infinity fluorometric plate reader with an excitation wavelength of 560 nm and emission of 590 nm.

Scheme 1. RAFT Polymerization of VPip Using 1 as CTA

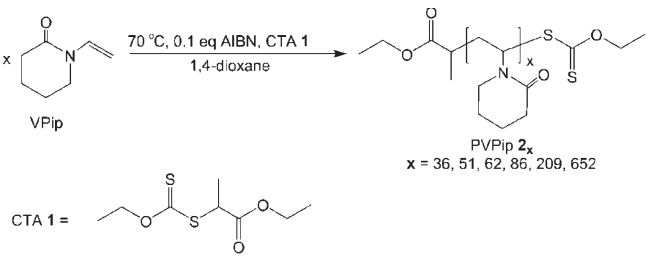

Results and Discussion

Reversible addition−fragmentation chain-transfer (RAFT) polymerization is a controlled radical polymerization technique which imparts living character to a conventional free radical polymerization by a degenerative chain-transfer mechanism via the use of a chain-transfer agent (CTA).[49−53] It has been well-documented that while RAFT agents such as trithiocarbonates and dithioesters can efficiently control the polymerization of more activated monomers (e.g., styrene, methacrylates), they are known to inhibit/retard the polymerization of the less activated monomers (e.g., vinyl acetate and *N*-vinyllactams).[51,54] On the other hand, xanthate and dithiocarbamate MADIX/RAFT agents which can effectively control the polymerizations of such less activated monomers tend to be inefficient with the more activated monomers.[55] As the ultimate goal of this work is to prepare a new class of thermally responsive block copolymer (namely PVPip-*b*-PVAc), the xanthate−ethyl 2-(ethoxycarbonothioylthio)propanoate (CTA **1**) was chosen as it is known to provide control over both vinyllactam[56] and the vinyl acetate[33,57] polymerizations.

The MADIX/RAFT of VPip monomer with **1** as a CTA in 1, 4-dioxane is shown in Scheme 1. A polymerization temperature of 70 °C was chosen as a compromise between the breakdown temperature of the xanthate CTA[58] and the reactivity of the PVPip propagating radical. At higher temperatures conversion of the monomer leveled out at ca. 60% (Figure S1), whereas at 70 °C a higher maximum conversion could be achieved, albeit with a decrease in polymerization rate. The ratio of **1**:AIBN initiator was kept at 1:0.1 to minimize the amount of active radicals present in the system and minimize the formation of dead chains while maintaining a reasonable rate of polymerization.[51]

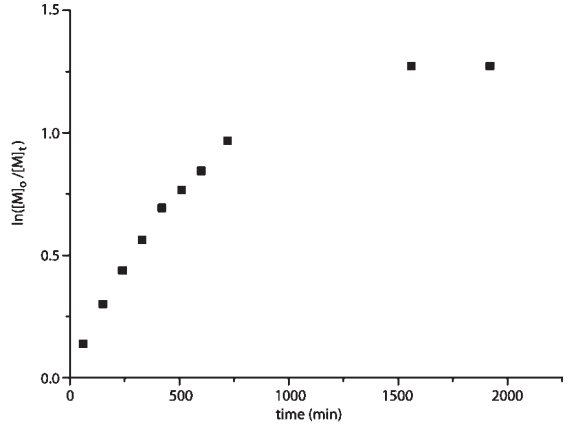

Figure 1. Pseudo-first-order kinetic plot for the solution polymerization of VPip (4 M in dioxane) at 70 °C using **1** as a CTA ([VPip]:[**1**]:[AIBN] = 160:1:0.1).

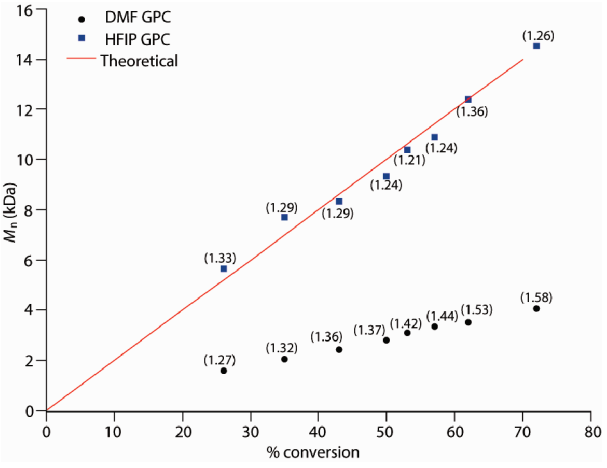

Figure 2. Evolution of M_n (HFIP GPC (blue squares) and DMF GPC (black dots), theoretical (red line)) with % conversion for the polymerization of VPip in 4 M dioxane with CTA **1** at 70 °C ([VPip]:[**1**]:[AIBN] = 160:1:0.1). M_w/M_n values are shown in parentheses.

Employing the above-mentioned conditions, the kinetics of the RAFT polymerization of VPip was then explored in detail. The controlled nature of the VPip RAFT polymerization ([VPip]:[**1**]:[AIBN] = 160:1:0.1) was confirmed by the pseudo-first-order kinetic plot as shown in Figure 1. It should be noted that linear kinetics were consistently observed only up to ca. 50% conversion and that in all cases the rate of polymerization leveled off after reaching ca. 70% (Figure 1). This was presumably due to a decomposition of the active radicals after prolonged heating as the polymerization proceeded. Furthermore, the apparent molecular weight (M_n^{GPC}, HFIP and DMF, Figure 2) was observed to increase linearly with conversion which is characteristic of a controlled polymerization system. Initial characterization of the polymer by GPC analysis using DMF as eluent constantly gave M_n values significantly lower than those obtained by NMR end-group and conversion analyses. This phenomenon has also been frequently observed in the 5-membered (poly(*N*-vinylpyrrolidone)) and the 7-membered (poly(*N*-vinylcaprolactam)) ring polymers.[35] To overcome this problem, we changed to use 1,1,-1,3,3,3-hexafluoro-2-propanol (HFIP) as eluent for our GPC analysis as it has been shown in the literature that molecular weight of polymers with very polar functional groups, e.g., polyamides and polyesters, could be analyzed using this system.[36] As anticipated, the apparent $M_n^{GPC,\ HFIP}$ were significantly higher than those obtained from DMF GPC when comparing

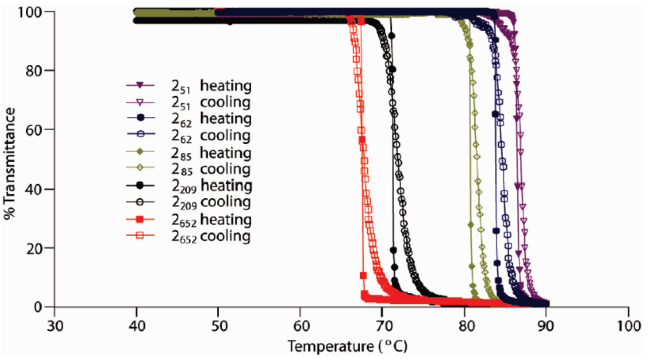

Figure 3. Percent transmittance versus temperature plots for $PVPip_x$ homopolymers of varying molecular weight at 20 mg/mL in water.

with the same standards. Furthermore, the M_n versus % conversion plot as analyzed by HFIP GPC agreed very well with the theoretical values. A series of homopolymers with control over M_n (4.5−83 kDa) were prepared by varying the monomer-to-CTA ratios taking into account the % conversion at which the polymerizations were quenched (Table S1). All the polymers obtained possessed fairly narrow molecular weight distributions as well as xanthate end groups as analyzed by a UV detector on the GPC (at 280 nm) (Figure S3). In addition, M_n values obtained from HFIP GPC also agreed relatively well with those from NMR end group and conversion analysis (Table S1, also see Figure S2 for a representative ^{1}H NMR spectrum of $\mathbf{2_{62}}$). The amorphous nature of PVPip could be confirmed by the DSC thermograms which showed glass transitions (T_g) at ca. 94−98 °C over the range of M_n's studied (4.5−83 kDa).

The cloud point behavior of these polymers in nanopure water was studied by turbidity measurements at 20 mg/mL. It has been well documented that while poly(*N*-vinylpyrrolidone) exhibited no phase separation behavior below 100 °C in water, its 7-membered ring analogue (poly(*N*-vinylcaprolactam)) had a cloud point of ca. 34 °C and hence has been compared with poly(*N*-isopropylacrylamide).[27,28] As expected, the range of cloud points of PVPip lay between those of its 5- and 7-membered ring polylactams (Figure 3). Furthermore, similar to other amide-based thermosensitive polymers (e.g., poly(2-oxazoline)), a chain length dependence on the cloud point was also observed with the cloud point decreasing with increasing molecular weight of the PVPip homopolymer (Figure S4).[26,59] Another interesting feature is that similar to poly(2-oxazolines) no hysteresis was evident from the overlapping heating and cooling traces in all phase transitions (Figure 3).[26]

To unambiguously prove that the PVPip homopolymers made by MADIX/RAFT polymerization have retained the xanthate end group functionality, they were chain extended with VAc, another "less activated monomer" which is known to polymerize in a controlled fashion using a xanthate CTA with identical Z-group as **1**.[33,57] In order to maximize the amount of dithiocarbonate end groups on the macro-CTA, the VPip homopolymerization was stopped at ca. 50% conversion when the kinetics was still linear. The molecular mass and polydispersity of $\mathbf{2_{62}}$ macro-CTA were determined by ^{1}H NMR end group and conversion analysis as well as GPC with HFIP and DMF as eluents. Both characterization techniques agreed reasonably well with each other (Table S1). The macro-CTA, $\mathbf{2_{62}}$, synthesized using the aforementioned optimized conditions was chain extended with VAc to make the amphiphilic block copolymer (PVPip-*b*-PVAc), with the ultimate aim being to study the thermal sensitive micellization behavior of this diblock copolymer (Scheme 2). Initial efforts to chain extend $\mathbf{2_{62}}$ in 4 M dioxane solution of VAc consistently yielded bimodal distributions by

Scheme 2. General Scheme of the Chain Extension of PVPip$_x$ with VAc at 60 °C in Dioxane To Obtain PVPip$_x$-*b*-PVAc$_y$

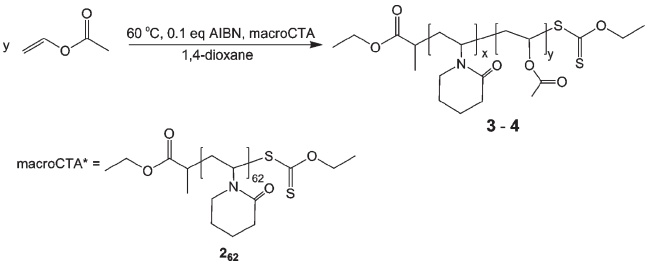

Table 1. Characterization of PVPip$_x$-*b*-PVAc$_y$ Synthesized from Macro-CTA 2$_{62}$ in This Study (*x* and *y* Denote the Degrees of Polymerization of Each Block)

block copolymer	*x*:*y*[a]	M_n^{HFIP}, kDa (M_w/M_n)[b]	M_n^{DMF}, kDa (M_w/M_n)[c]
3	62:21	10.7 (1.27)	4.4 (1.46)
4	62:32	11.4 (1.27)	7.4 (1.55)

[a] *x*:*y* was determined by comparing the −CH protons on the polymer backbones of the respective blocks (for PVPip δ (−C*H*−) 4.54 ppm, PVAc δ (−C*H*−) 4.84 ppm) and the $-CH_2$ protons on the heterocycle of the PVPip macro-CTA (δ (−NCH_2−) 3.02). [b] Determined from HFIP GPC calibrated with PMMA standards. [c] Determined from DMF GPC calibrated with PMMA standards.

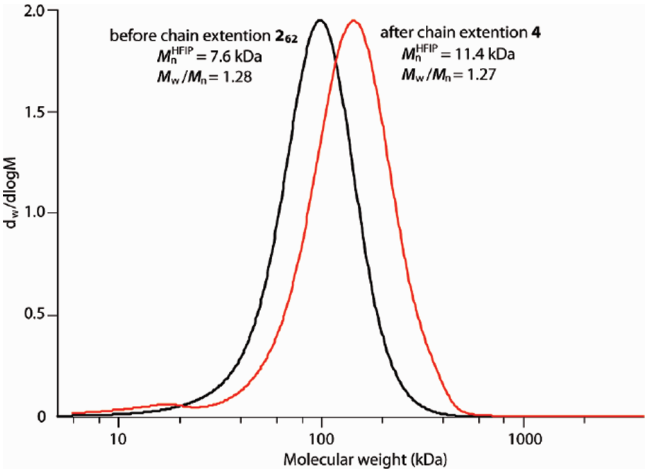

Figure 4. GPC (HFIP) trace of macro-CTA PVPip$_{62}$ and chain-extended diblock copolymer **4**.

GPC analysis. After attempting various reaction conditions which included different temperatures, solvents, and concentrations, it was found that a reasonably controlled polymerization could be achieved by lowering the concentrations (ca. 1 M VAc in dioxane) at 60 °C and by quenching the polymerizations at ca. 50% conversion. By adapting the optimized protocol, fairly well-defined amphiphilic PVPip$_x$-*b*-PVAc$_y$ diblock copolymers could be prepared (GPC (DMF), M_w/M_n 1.46−1.55, GPC (HFIP), M_w/M_n 1.27, Table 1).

The PVPip$_{62}$-*b*-PVAc$_{21/32}$ block copolymers (**3** and **4**) could be recovered by multiple precipitations into diethyl ether to yield white fluffy powders. The degrees of polymerization of the diblock copolymers were determined by comparing the integrations of the −C*H* protons on the polymer backbone of the respective blocks (for PVPip δ (−C*H*−) 4.54 ppm, PVAc δ (−C*H*−) 4.84 ppm), and the $-CH_2$ protons on the heterocycle of the PVPip macro-CTA (δ (−NCH_2−) 3.02) after purification (see Figure S5 for a representative ^{1}H NMR spectrum of **4**). Figure 4 shows the GPC traces (HFIP) before and after chain extension of PVPip$_{62}$ with VAc. A successful chain extension was

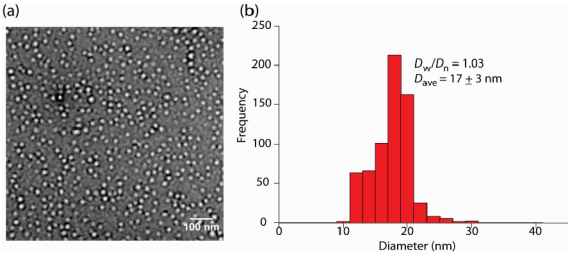

Figure 5. (a) Representative TEM image of spherical micelles obtained by deposition of a drop of an aqueous micelle solution (1 mg/mL) of **3** onto carbon-coated copper grids. The sample was stained with a 3% uranyl acetate solution prior to imaging. (b) Histogram of the size distribution of micelles obtained from **3** with size distribution (D_w/D_n).

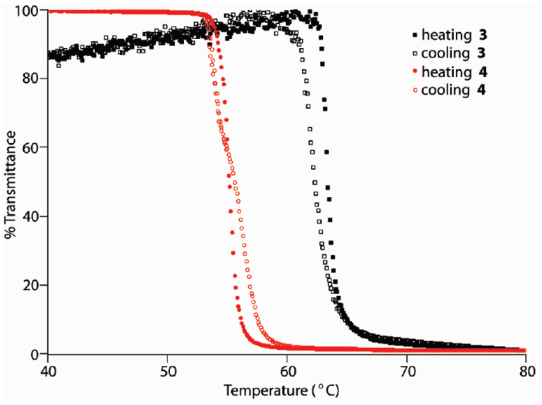

Figure 6. Plot of the % transmittance versus temperature (°C) for the diblock copolymers **3** and **4** (1 mg/mL) in nanopure water; heating and cooling rate = 1 °C/min.

apparent from the obvious shift toward higher molecular weight of the resulting diblock copolymer from that of the PVPip macro-CTA, thus further reinforcing the controlled nature of the PVPip homopolymerization.

The presence of a thermoresponsive hydrophilic PVPip block and a hydrophobic PVAc segment means that these copolymers can potentially be precursors to nanoparticles with a PVPip corona and a PVAc core upon dissolution in water—a selective solvent for the former block. The micellization behavior of PVPip$_{62}$-*b*-PVAc$_{21}$ **3** in nanopure water was studied by bright field transmission electron microscopy (TEM), atomic force microscopy (AFM), and dynamic light scattering (DLS). Because of the relatively long water-soluble PVPip block, self-assembly can be induced by directly dissolving the diblock copolymer in nanopure water (at 1 mg/mL).[60] The morphology and size of the self-assembled material were further investigated by TEM and DLS analysis (Figure 5 and Figure S6, respectively; also see Figure S7 for AFM images). DLS of the resulting clear solution confirmed that nanostructures of ca. 24 nm with quite broad polydispersity 0.523) were obtained with good correlation function (Figures S6(a) and S6(b), respectively). By DLS it appeared that some larger aggregates were also formed (as evidenced in the intensity profile), and attempts to optimize the assembly conditions (lower concentration, using a solvent switch method) could not prevent the formation of these larger aggregates. Analysis of the particles by TEM suggested spherical micelle diameters (ca. 17 ± 3 nm) which were smaller than those obtained from DLS measurements. However, discrepancies in size between the two characterization techniques is expected. It is likely that while DLS measured micellar sizes with a solvated PVPip corona in water, TEM images were likely to result in relatively smaller size due to the collapsed PVPip coronal chains upon drying on copper grids.

Scheme 3. Hydrolysis of 4 To Form 5

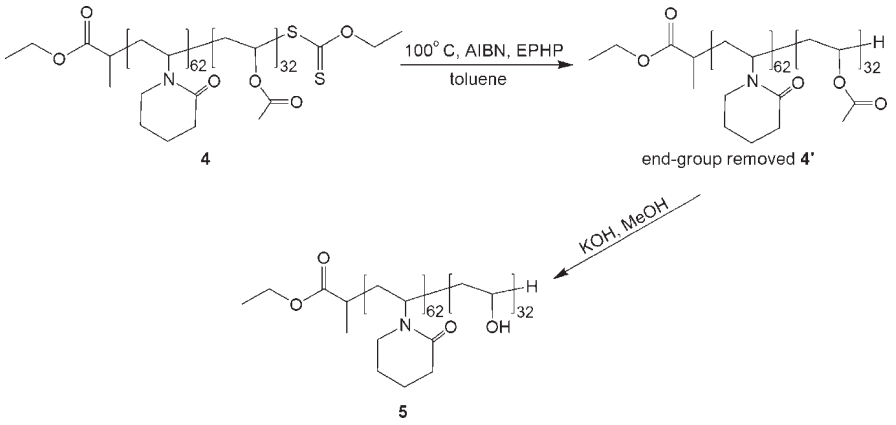

The formation of spherical micelle morphologies as confirmed by TEM analysis was consistent with the hydrophilic:hydrophobic block ratios of the PVPip-*b*-PVAc copolymer (Figure 5a). Furthermore, the size distributions (D_w/D_n 1.03) of these spherical micelles were fairly narrow as determined by TEM image analyses (Figure 5b). The critical aggregate concentration (CAC) of micellar **3** in nanopure water was also studied by fluorescence spectroscopy using *N*-phenyl-1-naphthylamine (PNA) as a fluorescent probe and was determined to be 8.8×10^{-3} mg/mL, which compares well with related amphiphilic systems (Figure S8).

The thermal sensitivity of these micellar structures was investigated by turbidity measurements. Figure 6 shows a plot of the % transmittance versus temperature profile for the micellar structures from **3** and **4**. It could be seen that in the case of **3** a sharp decrease in transmittance occurred at ca. 62 °C which signified a phase transition of the hydrophilic PVPip block. Analogous studies by DLS also showed that an abrupt increase in scattering intensity can be observed at ca. 62 °C (see Supporting Information Figure S9). Furthermore, upon cooling below the cloud point, micelles of **3** were readily reformed, demonstrating the reversibility of the phase transition. Interestingly, relative to the $PVPip_{62}$ homopolymer from which it was derived (cloud point of $PVPip_{62}$ ca. 84 °C), the cloud point of the corresponding diblock copolymer was significantly reduced. Furthermore, the sensitive copolymers phase transition of the diblock copolymer **4** (55 °C, Figure 6) in nanopure water was even lower than that of **3** (62 °C). We proposed that the observed decrease in cloud points of **3** and **4** relative to $\mathbf{2_{62}}$ from which they were derived could be attributed to the increase in hydrophobicity of the polymer due to the incorporation of the PVAc block. Similar behavior has also been observed in other amide-based thermal sensitive copolymers.[26] The heating and cooling traces overlaid reasonably well with each other, indicating the presence of only minimal hysteresis.

Recently, poly(*N*-vinylcaprolactam) and its derivatives have been extensively investigated due to their potential use in biomedical applications as a result of its nontoxic nature and an LCST close to body temperature.[29,43,61] It is anticipated that PVPip, the 6-membered ring structural analogue, should also be biocompatible and the LCST/cloud point of the polymer should be tunable by copolymerization with the 5- and 7-membered ring analogues. In our present study, we have also explored the cytotoxicity of PVPip, with the ultimate aim of making a fully biocompatible and thermoresponsive block copolymer: PVPip-*b*-PVOH. Cytotoxicity was measured using a LDH release assay. The LDH enzyme is released from the cell cytoplasm into the medium when cells have been lysed or have lost their membrane integrity. The released LDH then reduces NAD+ to NADH, which in turn is able to reduce the nonfluorescent rezazurin to the fluorescent resorufin. The dose response curve obtained for Calu-3 cells treated with $PVPip_{62}$ is shown in Figure S10. The polymer caused no significant deviation from the spontaneous LDH release even at the highest concentration of 1% w/v. Encouraged by the cytotoxicity data, we proceed into making $PVPip_{62}$-*b*-$PVOH_{32}$ in the hope of making a novel fully biocompatible block copolymer.

The hydrolysis of the PVAc block of **4** was performed under basic conditions in methanol. It has been well documented that by using this method, the PVPip block would remain intact while complete hydrolysis of the PVAc block could be readily achieved.[39,57] Previous reports have also suggested that a high molecular weight shoulder was occasionally observed (when analyzed by GPC) after hydrolysis. This was rationalized by the formation of disulfide end group functionalities which could ultimately lead to coupling of two polymer chains in the presence of oxygen.[62] To overcome this potential problem, we attempted to removed the xanthate end groups of **4** prior to hydrolysis employing a previously published method using ethylpyridine hypophosphite (EPHP) and AIBN (Scheme 3).[63] The end group removed polymer **4′** was then hydrolyzed using the conventional method as mentioned previously.[39,57] The successful formation of the diblock copolymer **5** was confirmed by the simultaneous disappearance of the $-CH_3$ signal (δ = 2.00 ppm) and the appearance of the $-CH-OH$ resonance (δ = 4.05 ppm) typical for PVOH (Figure S11). Furthermore, the selective hydrolysis of the PVAc block was supported by the fact that all ^{1}H NMR resonances corresponding to the PVPip block remained intact. This was further evidenced by the observation that upon hydrolysis the characteristic C=O stretch corresponding to the PVAc block disappeared while that of the PVPip block remained unchanged (Figure S12). Furthermore, the GPC RI traces (HFIP) showed that the hydrodynamic size of the block copolymer **4** was essentially unaffected after hydrolysis to form **5** (Figure S13). The thermoresponsive behavior of **5** in nanopure water was also investigated. It was anticipated that when an aqueous solution of **5** was heated above its cloud point, nanostructures with a water-soluble PVOH corona and a collapsed PVPip core should be formed. However, no apparent self-assembled micellar structures were detectable even after heating to 95 °C as monitored by changes in size and scattering intensity by DLS. It is likely that the increase in hydrophilicity upon hydrolysis of the PVAc segments and the apparent miscibility of the PVOH and PVPip blocks (as is suggested by the observation of a single T_g at 89 °C) prevent phase separation and nanostructure formation. The biocompatibility of this diblock copolymer was also confirmed using methods employed for the homopolymer derivative. Importantly, this result further reinforced our earlier observations with the block copolymers **3** and **4** that the cloud point of the final material can be easily tuned by altering the hydrophilicity/hydrophobicity of the diblock.

Conclusions

This paper reports for the first time the synthesis of the novel biocompatible and thermoresponsive polymer PVPip by MADIX/RAFT polymerization using xanthate **1** as a chain-transfer agent. The cloud points of these polymers were shown to be chain length dependent, and the transitions were observed to be reversible and fast. Furthermore, cell toxicity studies on $\mathbf{2}_{62}$ indicated that the PVPip is noncytotoxic even at high dosage levels (1% w/v). Amphiphilic diblock copolymers **3** and **4** have been successfully prepared by chain extending from the macro-CTA $\mathbf{2}_{62}$ with VAc. The self-assembly of **3** into thermoresponsive spherical micelles could easily be induced by direct dissolution in nanopure water and have been fully characterized by DLS, TEM, and AFM. Moreover, spherical micelles of **3** exhibited a cloud point which could be further tuned by changing the hydrophobic PVAc block length. A fully biocompatible block copolymer $PVPip_{62}$-*b*-$PVOH_{32}$ **5** was also prepared by basic hydrolysis of **4**. Our results suggest that PVPip polymer not only possesses excellent potential as a novel thermosensitive biomaterial in its own right, but the possibility of copolymerizing with its 5- and 7-membered ring analogues may give rise to tunable LCST polymers with novel properties.

Acknowledgment. The authors acknowledge the Royal Society, EPSRC, and the University of Warwick for funding. The GPCs used in this research were obtained, through Birmingham Science City: Innovative Uses for Advanced Materials in the Modern World (West Midlands Centre for Advanced Materials Project 2), with support from Advantage West Midlands (AWM) and part funded by the European Regional Development Fund (ERDF). The authors also thank Dr. Helen Willcock for assistance with GPC measurements, Mr. Joseph Patterson for DSC measurements, Mr. Daniel Le Huray for initial work on VPip, and Dr. Matthew Gibson for helpful discussions. We also thank BASF for donation of the VPip monomer.

Supporting Information Available: Further polymer and micelle characterization and biocompatibility data. This material is available free of charge via the Internet at http://pubs.acs.org.

References and Notes

(1) Dai, S.; Ravi, P.; Tam, K. C. *Soft Matter* **2009**, *5*, 2513–2533.
(2) de las Heras Alarcón, C.; Pennadam, S.; Alexander, C. *Chem. Soc. Rev.* **2005**, *34*, 276–285.
(3) Alexander, C.; Shakesheff, K. M. *Adv. Mater.* **2006**, *18*, 3321–3328.
(4) Gil, E. S.; Hudson, S. M. *Prog. Polym. Sci.* **2004**, *29*, 1173–1222.
(5) Schmaljohann, D. *Adv. Drug Delivery Rev.* **2006**, *58*, 1655–1670.
(6) Bajpai, A. K.; Shukla, S. K.; Bhanu, S.; Kankane, S. *Prog. Polym. Sci.* **2008**, *33*, 1088–1118.
(7) Onaca, O.; Enea, R.; Hughes, D. W.; Meier, W. *Macromol. Biosci* **2009**, *9*, 129–139.
(8) Moughton, A. O.; O'Reilly, R. K. *Chem. Commun.* **2010**, 1091–1093.
(9) Kikuchi, A.; Okano, T. *Prog. Polym. Sci.* **2002**, *27*, 1165–1193.
(10) Chan, G.; Mooney, D. J. *Trends Biotechnol.* **2008**, *26*, 382–392.
(11) Taylor, L.; Cerankowski, L. D. *J. Polym. Sci.* **1975**, *13*, 2551–2570.
(12) Heskins, J.; Guillet, J. E. *J. Macromol. Sci., Part A: Pure Appl. Chem.* **1968**, *2*, 1441–1455.
(13) Schild, H. G. *Prog. Polym. Sci.* **1992**, *17*, 163–249.
(14) Feil, H.; Bae, Y. H.; Feijen, J.; Kim, S. W. *Macromolecules* **1993**, *26*, 2496–2500.
(15) Furyk, S.; Zhang, Y.; Ortiz-Acosta, D.; Cremer, P. S.; Bergbreiter, D. E. *J. Polym. Sci., Part A: Polym. Chem.* **2006**, *44*, 1492–1501.
(16) Xia, Y.; Burke, N. A. D.; Stöver, H. F. H. *Macromolecules* **2006**, *39*, 2275–2283.
(17) Kujawa, P.; Segui, F.; Shaban, S.; Diab, C.; Okada, Y.; Tanaka, F.; Winnik, F. M. *Macromolecules* **2006**, *39*, 341–348.
(18) Han, S.; Hagiwara, M.; Ishizone, T. *Macromolecules* **2003**, *36*, 8312–8319.
(19) Zhao, B.; Li, D.; Hua, F.; Green, D. R. *Macromolecules* **2005**, *38*, 9509–9517.
(20) Lutz, J.-F.; Akdemir, Ö.; Hoth, A. *J. Am. Chem. Soc.* **2006**, *128*, 13046–13047.
(21) Lutz, J.-F.; Hoth, A. *Macromolecules* **2006**, *39*, 893–896.
(22) Lutz, J.-F.; Andrieu, J.; Üzgün, S.; Rudolph, C.; Agarwal, S. *Macromolecules* **2007**, *40*, 8540–8543.
(23) Okada, M.; Aoi, K. *Prog. Polym. Sci.* **1996**, *21*, 151–208.
(24) Park, J.-S.; Kataoka, K. *Macromolecules* **2006**, *39*, 6622–6630.
(25) Huber, S.; Jordan, R. *Colloid Polym. Sci.* **2008**, *286*, 395–402.
(26) Hoogenboom, R.; Thijs, H. M. L.; Jochems, M. J. H. C.; van Lankvelt, B. M.; Fijten, M. W. M.; Schubert, U. S. *Chem. Commun.* **2008**, 5758–5760.
(27) Maeda, Y.; Nakamura, T.; Ikeda, I. *Macromolecules* **2002**, *35*, 217–222.
(28) Laukkanen, A.; Valtola, L.; Winnik, F. M.; Tenhu, H. *Macromolecules* **2004**, *37*, 2268–2274.
(29) Lau, A. C. W.; Wu, C. *Macromolecules* **1999**, *32*, 581–584.
(30) Meeuseeen, F.; Nies, E.; Berghmans, H.; Verbrugghe, S.; Goethals, E.; Du Prez, F. *Polymer* **2000**, *41*, 8597–8602.
(31) Devasia, R.; Bindu, R. L.; Borsali, R.; Mougin, N.; Gnanou, Y. *Macromol. Symp.* **2005**, *229*, 8–17.
(32) Wan, D.; Satoh, K.; Kamigaito, M.; Okamoto, Y. *Macromolecules* **2005**, *38*, 10397–10405.
(33) Pound, G.; Aguesse, F.; McLeary, J. B.; Lange, R. F. M.; Kulmperman, B. *Macromolecules* **2007**, *40*, 8861–8871.
(34) Pound, G.; Eksteen, Z.; Pfukwa, R.; McKenzie, J. M.; Lange, R. F. M.; Klumperman, B. *J. Polym. Sci., Part A: Polym. Chem.* **2008**, *46*, 6575–6593.
(35) Wan, D.; Zhou, Q.; Pu, H.; Yang, G. *J. Polym. Sci., Part A: Polym. Chem.* **2008**, *46*, 3756–3765.
(36) Fandrich, N.; Falkenhagen, J.; Weidner, S. M.; Pfeifer, D.; Staal, B.; Thünemann, A. F.; Laschewsky, A. *Macromol. Chem. Phys.* **2010**, *211*, 869–878.
(37) Bilalis, P.; Pitsikalis, M.; Hadjichristidis, N. *J. Polym. Sci., Part A: Polym. Chem.* **2006**, *44*, 659–665.
(38) Lu, X.; Gong, S.; Meng, L.; Li, C.; Yang, S.; Zhang, L. *Polymer* **2007**, *48*, 2835–2842.
(39) Debuigne, A.; Willet, N.; Jérôme, R.; Detrembleur, C. *Macromolecules* **2007**, *40*, 7111–7118.
(40) Loos, W.; Verbrugghe, S.; Goethals, E. J.; Du Prez, F. E.; Bakeeva, I. V.; Zubov, V. P. *Macromol. Chem. Phys.* **2003**, *204*, 98–103.
(41) Shtanko, N. I.; Lequieu, W.; Goethais, E. J.; Du Prez, F. E. *Polym. Int.* **2003**, *52*, 1605–1610.
(42) Aseyev, V.; Hietala, S.; Laukkanen, A.; Nuopponen, M.; Confortini, O.; Du Prez, F. E.; Tenhu, H. *Polymer* **2005**, *46*, 7118–7131.
(43) Prabaharan, M.; Grailer, J. J.; Steeber, D. A.; Gong, S. *Macromol. Biosci.* **2009**, *9*, 744–753.
(44) Shah, S.; Pal, A.; Gude, R.; Devi, S. *Eur. Polym. J.* **2010**, *46*, 958–967.
(45) Yan, N.; Zhang, J.; Yuan, Y.; Chen, G.-T.; Dyson, P. J.; Li, Z.-C.; Kou, Y. *Chem. Commun* **2010**, *46*, 1631–1633.
(46) Kizhnyaev, V. N.; Krakhotkina, E. A.; Petrova, T. L.; Ratovskii, G. V.; Tyukalova, O. V.; Pokatilov, F. A.; Smirnov, A. I. *Polym. Sci., Ser. B* **2010**, *52*, 480–486.
(47) Skey, J.; O'Reilly, R. K. *Chem. Commun* **2008**, 4183–4185.
(48) Aikyoshi, K.; Deguchi, S.; Moriguchi, N.; Yamaguchi, S.; Sunamoto, J. *Macromolecules* **1993**, *26*, 3062–3068.
(49) Moad, G.; Rizzardo, E.; Thang, S. H. *Polymer* **2008**, *49*, 1079–1131.
(50) Moad, G.; Rizzardo, E.; Thang, S. H. *Aust. J. Chem.* **2006**, *59*, 669–692.
(51) Moad, G.; Rizzardo, E.; Thang, S. H. *Aust. J. Chem.* **2005**, *58*, 379–410.
(52) Chiefari, J.; Chong, Y. K. B.; Ercole, F.; Krstina, J.; Jeffery, J.; P. T. Le, T.; Mayadunne, R. T. A.; Meijs, G. F.; Moad, C. L.; Moad, G.; Rizzardo, E.; Thang, S. H. *Macromolecules* **1998**, *31*, 5559–5562.
(53) Willcock, H.; O'Reilly, R. K. *Polym. Chem.* **2010**, *1*, 149–157.
(54) Perrier, S.; Takolpuckdee, P. *J. Polym. Sci., Part A: Polym. Chem.* **2005**, *43*, 5347–5393.
(55) Benaglia, M.; Chiefari, J.; Chong, Y. K.; Moad, G.; Rizzardo, E.; Thang, S. H. *J. Am. Chem. Soc.* **2009**, *131*, 6914–6915.
(56) Devasia, R.; Bindu, R. L.; Mougin, N.; Gnanou, Y. *Polym. Prepr.* **2005**, *46* (2), 195–196.
(57) Stenzel, M. H.; Davis, T. P.; Barner-Kowollik, C. *Chem. Commun* **2004**, 1546–1547.

(58) Legge, T. M.; Slark, A. T.; Perrier, S. *J. Polym. Sci., Part A: Polym. Chem.* **2006**, *44*, 6980–6987.
(59) Liu, S.; Jiang, M.; Liang, H.; Wu, C. *Polymer* **2000**, *41*, 8697–8702.
(60) Zhang, L.; Eisenberg, A. *J. Am. Chem. Soc.* **1996**, *118*, 3168–3181.
(61) Prabaharan, M.; Grailer, J. J.; Steeber, D. A.; Gong, S. *Macromol. Biosci.* **2008**, *8*, 843–851.
(62) Bernard, J.; Favier, A.; Zhang, L.; Nilasaroya, A.; Davis, T. P.; Barner-Kowollik, C.; Stenzel, M. H. *Macromolecules* **2005**, *38*, 5475–5484.
(63) Moughton, A. O.; Stubenrauch, K.; O'Reilly, R. K. *Soft Matter* **2009**, *5*, 2361–2370.